IOP PUBLISHING JOURNAL OF PHYSICS D: APPLIED PHYSICS

J. Phys. D: Appl. Phys. **46** (2013) 385103 (6pp) doi:10.1088/0022-3727/46/38/385103

The stress-affected carrier injection and transport in organic semiconductor devices

Weifeng Dai[1], Bin Zhang[2], Yonglong Kang[1], Huamin Chen[1], Gaoyu Zhong[1], Yuesheng Li[1]

[1] Department of Materials Science, Fudan University, Shanghai 200433, People's Republic of China
[2] CSM Instruments SA, CH-2034 Peseux, Switzerland

E-mail: gyzhong@fudan.edu.cn

Received 11 March 2013, in final form 16 July 2013
Published 4 September 2013
Online at stacks.iop.org/JPhysD/46/385103

Abstract

The current–voltage (I–V) characteristics of the thin films of methoxy-5-(2'-ethylhexyloxy)-1,4-phyenylenevinylene] (MEH-PPV) and tris-(8-hydroxyquinoline) aluminum (Alq) under different stresses have been measured, together with their Young's modulus, hardness, and loading curve. We propose a model on stress-affected carrier injection and transport to explain the experimental results. The model is based on the well-built space-charge-limited current (SCLC) and injection-limited current (ILC) model, together with the electrical and mechanic properties of organic semiconductor. By Monte Carlo simulation, we investigated the relationship between the conductance and strain. We found two trends in the current variation with the stress. One is fast at low current density, and the other is relatively slower at high current density, which may due to the SCLC in the bulk and the ILC at the interface, respectively. The working voltage of the present device with the highest sensitivity is about 1 V.

(Some figures may appear in colour only in the online journal)

1. Introduction

The possibility of organic semiconductor applied as the sensing material in stress sensor has been well demonstrated by researchers [1–6]. The organic semiconductors, especially some polymers, including methoxy-5-(2'-ethylhexyloxy)-1,4-phyenylenevinylene] (MEH-PPV), show a high sensitivity, good repeatability, and fast responsibility in stress sensing. This should be due to the fact that the solid thin films of organic semiconductor are usually bonded by molecular bond (Van der Waals force). The moderately big intermolecular space can easily be compressed, and the compression would result in a remarkable increasing of conductance. Thus, the resistance of the organic thin film would change with the applied stress apparently. This is the named piezoresistance effect [7, 8].

We have proposed two mechanisms in an organic piezoresistance device. One is that the carriers in the bulk would hop from site to site under the Miller–Abrahams model [4, 9, 10]. The other is that the macromolecular conjugated chain changes to be a micro-passway of current when a polymer is compressed [5]. Though the two mechanisms revealed some phenomena on the piezoresistance behaviour of the organic thin films, the important effect of interface and the related carrier injection have not both been considered. It is well known that the interface plays a very important role in such a thin film, thus the carrier injection at the interface should be considered in its piezoresistance.

In the present study, we propose a model of conductance varying with the applied stress. Based on the experimental and the simulation, we explained the piezoresistance effect of organic semiconductor film. It is conclude that, in the present organic piezoresistive device, the current is mainly limited by two factors. One factor is the carrier injection. It would affect the current more seriously than the carrier transport in the bulk if the bulk resistance of the film is low; the other factor is the carrier transport, which would play a more important role when sufficient carriers are injected. The two factors would be effective simultaneously, but show different influences on stress sensing under the low or high current density.

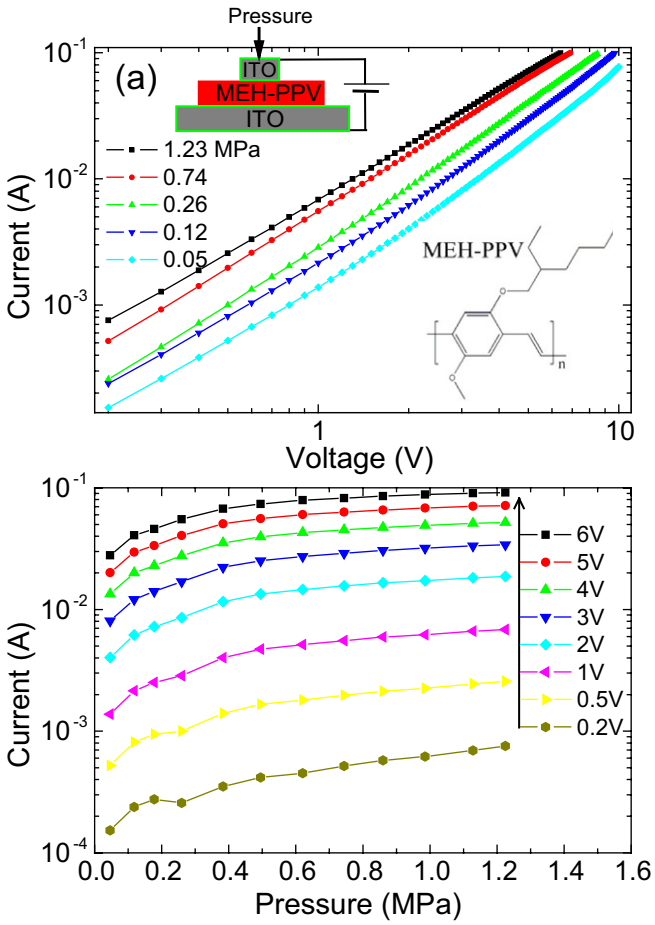

Figure 1. The I–V characteristics of a sensor under different stress (a), including the inset device structure ITO/MEH-PPV/ITO and the molecular structure of MEH-PPV, together with the current varying with the applied stress at different voltages in the same experiment (b).

2. Experimental details

We fabricated the piezoresistive devices with tris-(8-hydroxyquinoline) aluminum (Alq) and MEH-PPV, and measured the I–V curve under different loads. The experimental details on Alq devices have been reported in our previous paper [4]. The experiments on MEH-PPV devices are detailed below. The molecular structure of MEH-PPV and the schematic diagram of the experimental set are shown in figure 1(a). The devices consisted of a single layer of MEH-PPV which is sandwiched between two indium tin oxide (ITO) electrodes. The ITO-deposited Si wafer substrates were sequentially cleaned in acetone, ethanol, and de-ionized water, and then exposed to oxygen plasma for 5 min. Polymer films were prepared on the ITO–Si substrates by spin-coating MEH-PPV dissolved in chloroform (5 mg ml^{-1}) at 1000 rpm for 60 s, which produced a uniform film with a thickness of ~120 nm. Force was applied to another small and clean ITO–Si substrate placed atop the MEH-PPV film using a probe tip attached to a micropositioner. To avoid the ITO–Si piece flexing and the related influence on measurement, the probe tip is put on the centre of the Si piece, while the force is no bigger than 1.5 kg, and the size of the ITO–Si piece was only $2 \times 3\,\mathrm{mm}^2$, which defined the active area of the sensors. The surfaces of the MEH-PPV film and the ITO–Si piece are very smooth. Both of them have a roughness better than several nanometres, and the MEH-PPV film is very soft. Therefore, a very small stress (<30 kPa) would result in a complete and uniform contact between them, which can be found through the measured stable, reliable, and repeatable I–V characteristics. The applied force was measured using an electronic precision balance with 0.1 g readability. The I–V characteristics of the devices were recorded using a Keithley 238 high-current source-measure unit. The base resistance of the set Si–ITO–ITO–Si (no MEH-PPV) is ~60 Ω, which would not change markedly with the applied stress. The stress–strain curves are measured using the ultra-nano indentation (UNHT) of CSM Instruments, with a 40 μm diameter flat punch and loading mainly with sinus model.

3. Results and discussion

Figure 1(a) shows the current varying with the voltage at different stress. The inset shows the device structure and the molecular structure of MEH-PPV. Figure 1(b) shows the current varying with stress at different voltages in the same experimental. It can be seen that the current is very sensitive to the applied stress. From the calculated slope of the $\log I$–$\log V$ plot, we found that it changes from 1.75 to 1.46 when the pressure changes from 0.05 to 1.23 MPa at the range of 2–10 V, while it remains 1.4–1.5 at the range of 0.2–1 V. That means its conductive mechanism changes from the space-charge-limited current (SCLC)-model-like to the Ohm's-law-like (the theoretical value of the slope in SCLC-model is 2, while it is 1 in Ohm's-law) when the material is compressed and the current density is big enough [19]. Based on the above experimental results, we try to construct a physical model, and simulate these results to explain the mechanism in the organic semiconductor piezoresistive sensors.

In the organic semiconductors, carriers hop between adjacent highest occupied molecular orbitals (HOMOs) or highest unoccupied molecular orbitals (LUMOs). The charge transfer process is different from inorganic semiconductors. Many models have been developed for describing the charge transfer in organic semiconductors, such as Marcus's electron transfer theory [11], the multiple-trapping model [12], and the Miller–Abrahams model [13]. In this work, we simulate the device current using Monte Carlo method based on the Miller–Abrahams model.

According to the Miller–Abrahams model [4, 9, 10], the probability of carrier hopping (ν_{ij}) from the ith local state to the jth local state is determined by the distance between local states (r_{ij}) and the energy difference ($\Delta E = E_j - E_i$):

$$\nu_{ij} = \nu_0 \mathrm{e}^{-\frac{2r_{ij}}{R}} \begin{cases} \mathrm{e}^{-\frac{E_j - E_i}{kT}} & (E_j > E_i) \\ 1 & (E_j \leqslant E_i), \end{cases} \quad (1)$$

where ν_0 is the constant of hopping probability which means the vibration frequency of phonons [14] and R is a constant which indicates the coupling distance between the two local states. When the destination energy level is higher, a phonon

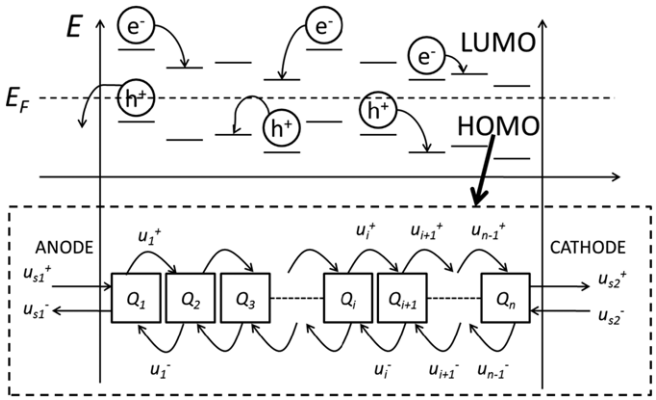

Figure 2. Sketch of the carrier hopping in organic semiconductor film.

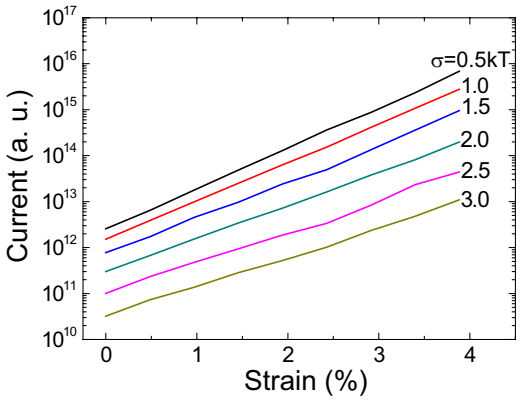

Figure 3. The simulation results of the current–strain relationship in the device with different energy disorders.

with energy of ΔE would be absorbed from the external environment. In the opposite case, a phonon with ΔE energy would be released. The hopping probability from the ith to the jth state is asymmetrical with that from the jth to the ith state.

The orientation and arrangement of organic molecules are not completely ordered. Therefore, the energy of the same molecular orbitals in different molecules is not a constant. Bässler *et al* [15] proposed a Gaussian disorder model and empirical formulations to estimate several characteristics in organic semiconductors.

Figure 2 shows schematically the disorder in the energy states of molecules and implies the carrier transporting process in energy scope (top). The Y-axis shows the energy and the X-axis shows the space coordinate in the thickness orientation. Figure 2 shows schematically at the bottom of the dashed frame that most of the electrons 'e' moved on the LUMOs from cathode to anode, while most holes 'h' moved on the HOMOs from anode to cathode. The LUMO and HOMO are localized with varying energy levels in accordance with the thermal distribution rules [15]. The present 1D model for the charge transport in the organic films is simple. Here Q_i is the carrier density of the ith molecular layer, u_i^+ is the mean rate of carrier moving from the ith layer to the $(i+1)$th layer, while u_i^- is that in the opposite direction.

The details of Monte Carlo simulation are described as follows. In the case of an Alq device, a simple-cubic crystal structure is applied to the molecular grids and 2D periodic boundary condition on the film plane is adopted. The thickness of Alq layer is about 80 nm and the equivalent crystal constant is estimated to be 1 nm [16, 17]. The applied working voltage is about 0.5–5 V and other strong tunnelling effect under high electric field can be omitted [18, 19]. Although the Joule's heating effect is an important factor in charge transport [20], we still set the working temperature to be 300 K (RT) for simplification. Gaussian disorder model [15] is adopted in our simulation. So the energy can be written as:

$$E_i^* = E_i + \theta \cdot kT, \tag{2}$$

where θ is dimensionless and random, which is a parameter in the following Gaussian distribution:

$$p(\theta)\,\mathrm{d}\theta = \frac{1}{\sqrt{2\pi\sigma^2}} \mathrm{e}^{-\frac{\theta^2}{2\sigma^2}}\,\mathrm{d}\theta. \tag{3}$$

Here σ is the standard deviation in the Gaussian distribution.

Figure 3 illustrates the simulation results of the current–strain relationship in the device with different energy disorders. The energy disorder will not change the exponential form of the current function on strain. The energy disorder affects the absolute current value and a little change of current increase with the increased strain. The energy disorder can be treated as a constant in a given organic semiconductor, as done in the present study.

The total current of the device consists of two parts: the diffusion current and the drift current:

$$J = q\left(-D\nabla n + n\mu E\right). \tag{4}$$

If the charge injection at the interface is sufficient and the energy disorder is small enough, the charge density will approach a constant and the diffusion current could be ignored. Then the drift current is controlled only by the properties of organic semiconductor materials. Because the mobility of carrier is proportioned to its hopping rate between two local states, the current density is an exponential function of strain, equation (8).

$$j = Q \cdot \left(u^+ - u^-\right) \propto \nu_{ij} - \nu_{ji}, \tag{5}$$

$$\nu_{ij} - \nu_{ji} = \nu_0 \mathrm{e}^{2\frac{|r-r_0|}{R}}, \tag{6}$$

$$j \propto \mathrm{e}^{\frac{|r-r_0|}{R/2}} = \mathrm{e}^{\left|\frac{r-r_0}{r_0}\right| / \frac{R}{2r_0}}. \tag{7}$$

So the current density j can be written as:

$$j = j_0 \mathrm{e}^{\frac{\varepsilon_z}{A}}, \tag{8}$$

where ε_z is the component of normal strain in the z-direction.

However, the experimental results show that the current tends to saturate if the stress increases to a certain value. The total current cannot always grow exponentially as described in equation (8). Two factors will suppress the current growth obviously: one is the nonlinearity of the stress–strain relationship; the other is the limited charge injection. In the present case, as shown in figure 4, the stress is so low that the stress–strain curve of MEH-PPV (a) seems linear in the

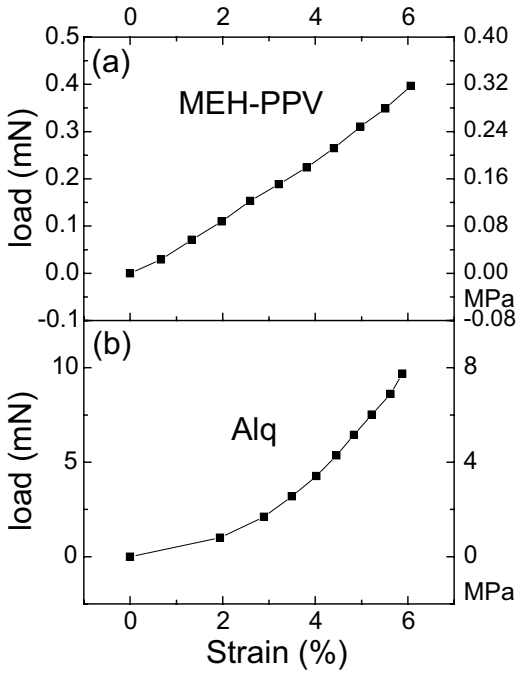

Figure 4. The stress–strain curves of MEH-PPV (*a*) and Alq (*b*) films.

measuring range. Thus, the nonlinearity of the stress–strain relationship may have less importance in this case. The stress–strain curve of Alq (*b*) is approaching nonlinear. The different linearity of stress–strain relationship may due to the fact that MEH-PPV is polymeric while Alq is small molecular. When the stress increases, the distance between two neighbouring sites will decrease, making the carrier hopping easier, so the carrier mobility is enhanced. While the carrier transports faster, the injection tends to be insufficient. Thus, the limited charge injection will become the main factor of suppressing current growth with the applied stress at a high current density.

As shown in figure 5, the carrier distribution built in the organic film is sketched schematically. It will vary with the electric field strength, and usually be distributed exponentially near the interface [21]. To establish the model for explaining the total current, some variables are introduced below: Q_0, equilibrium carrier density without voltage; Q_1 and Q_2, carrier densities at the interfaces in organic; q_1 $(= Q_1 - Q_0)$ and $q_2(= Q_2 - Q_0)$, the differences of carrier densities at the interfaces in organic; $u_{s1}^+, u_{s1}^-, u_{s2}^+, u_{s2}^-$, hopping rates of carriers at the interfaces; L, thickness of the organic film.

At the electrode–organic interfaces, the charge injection would be strongly affected by the alignment of energy level. According to figure 5, the current injected by interfacial charges is given below:

$$j = \begin{cases} j_{s1} = -(Q_1 - Q_0)\, u_{s1}^- = q_1 u_{s1}^- \\ j_{s2} = (Q_2 - Q_0)\, u_{s2}^+ = q_2 u_{s2}^+. \end{cases} \tag{9}$$

The current inside device is:

$$j = j_i = Q_i u_i^+ - Q_{i+1} u_{i+1}^-, \tag{10}$$

Q_i is the mean carrier density of the ith molecular layer (simple-cubic lattice) and u_i is the mean transfer rate of the

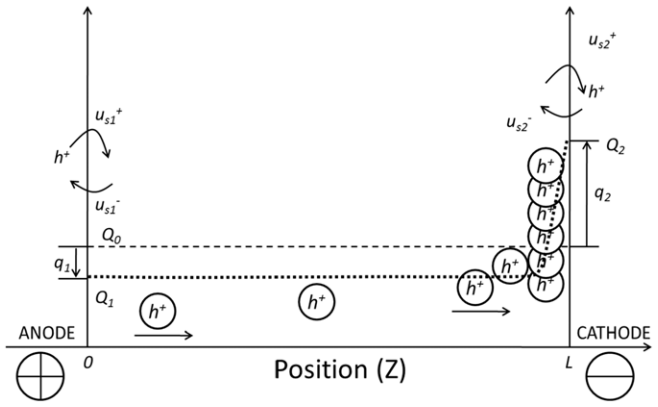

Figure 5. Sketch of carrier (hole) injection and the carrier distribution (plot in a logarithmic scale) built in the organic film.

ith molecular layer. Here, u is a function of strain. Applying the Miller–Abrahams model to the transfer process [4, 9, 10], we have:

$$u^+ = u^- \mathrm{e}^{\frac{\Delta E}{kT}}, \tag{11}$$

$$\frac{\Delta Q_{i+1}}{\Delta Q_i} = \frac{u^+}{u^-} = \mathrm{e}^{\frac{\Delta E}{kT}}, \tag{12}$$

ΔE is the mean energy difference between the two adjacent molecular layers, and $\Delta Q_i (= Q_{i+1} - Q_i)$ is the carrier density difference between these two layers. Associating with $Q_n - Q_1 = \sum_{i=1}^{n-1} \Delta Q_i = q_1 + q_2$ and $j_{s1} = j_{s2}$, we obtain:

$$\Delta Q_1 = q_1 \left(1 + \frac{u_{s1}^-}{u_{s2}^+}\right) \frac{1 - \frac{u^+}{u^-}}{1 - \left(\frac{u^+}{u^-}\right)^{n-1}}, \tag{13}$$

$$j = Q_1 u^+ - (Q_1 + \Delta Q_1)\, u^- = Q_1 \left(u^+ - u^-\right) - \Delta Q_1 u^-. \tag{14}$$

In equation (14), the first part $Q_1 \left(u^+ - u^-\right)$ is the drift current, and the last part $-\Delta Q_1 u^-$ is the diffusion current. In equation (13), since

$$\frac{1 - \frac{u^+}{u^-}}{1 - \left(\frac{u^+}{u^-}\right)^{n-1}} \sim 10^{-8}$$

(calculated using the parameters 0.5 V and 80 nm thickness), and $(u_{s1}^-/u_{s2}^+) \sim 1$ (assuming the anode and cathode are similar), the diffusion current near anode (for hole) can be ignored.

Considering u is a function of Δz or strain ε_z, we obtain the current–strain relation by applying the Miller–Abrahams model on interfacial charge transfer process (the reason discussed below) and substituting parameter B for A in equation (8):

$$j\,(\varepsilon_z) = Q_0 u_{s1}^- \mathrm{e}^{\frac{\varepsilon_z}{B}} \frac{\mathrm{e}^{\frac{\varepsilon_z}{A}}}{\mathrm{e}^{\frac{\varepsilon_z}{A}} + \frac{u_{s1}^-}{u^+ - u^-} \mathrm{e}^{\frac{\varepsilon_z}{B}}}. \tag{15}$$

We can set $C = (u_{s1}^-/u^+ - u^-)$ as the ratio of interfacial transfer rate to the net transfer rate along z-axis, equation (15) becomes:

$$j\,(\varepsilon_z) = Q_0 \left(u^+ - u^-\right) \cdot C \mathrm{e}^{\frac{\varepsilon_z}{B}} \frac{\mathrm{e}^{\frac{\varepsilon_z}{A}}}{\mathrm{e}^{\frac{\varepsilon_z}{A}} + C \mathrm{e}^{\frac{\varepsilon_z}{B}}}. \tag{16}$$

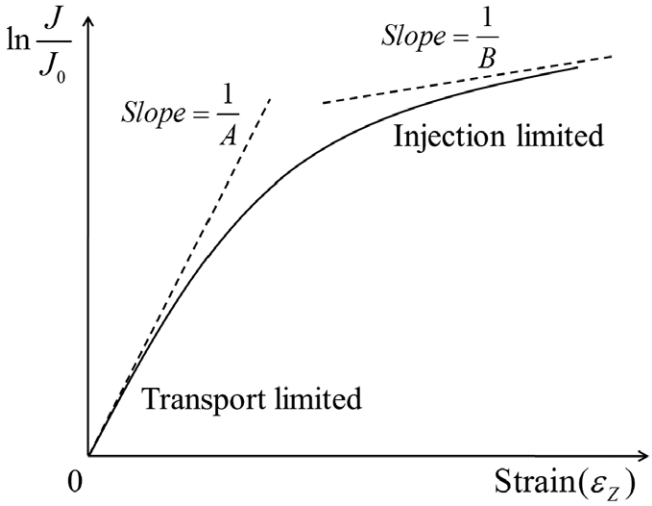

Figure 6. The schematic tendency of current varying with strain ($\ln(j(\varepsilon_z)/j(0)) \sim \varepsilon_z$).

Assuming the parameter B is much larger than A (the reason is given below), two asymptotes are given in the curve of $\ln \frac{j(\varepsilon_z)}{j(0)} \sim \varepsilon_z$ (see figure 6) according to equation (16):

$$\ln \frac{j(\varepsilon_z)}{j(0)} = \ln\left(\mathrm{e}^{\frac{\varepsilon_z}{B}} \frac{\mathrm{e}^{\frac{\varepsilon_z}{A}}}{\mathrm{e}^{\frac{\varepsilon_z}{A}} + C\mathrm{e}^{\frac{\varepsilon_z}{B}}}\right) = \begin{cases} \frac{\varepsilon_z}{A} + \frac{\varepsilon_z}{B} \approx \frac{\varepsilon_z}{A}, & \left(\frac{\varepsilon_z}{A} \ll C\mathrm{e}^{\frac{\varepsilon_z}{B}}\right) \\ \frac{\varepsilon_z}{B}, & \left(\frac{\varepsilon_z}{A} \gg C\mathrm{e}^{\frac{\varepsilon_z}{B}}\right), \end{cases} \tag{17}$$

where A and B indicate the critical strain value at which the stress markedly affects the carrier transport and injection, respectively.

In the present work, as the strain is larger than A, it would result in a significant increase of current, which is due to the strong enhancement of carrier transport. And when the strain increases to a big value of B, the current will be too big to get sufficient carriers from the organic/electrode interface. So the carrier injection would become the critical factor which limits the current.

Based on equation (16), two asymptotic lines can be figured out. It can be seen that when the stress and strain are low, the current density is also low. Then the current variation is dominated by the carrier's bulk transport. While the carrier injection at the interface is sufficient, the main trouble for the carrier is to overcome the intermolecular energy barrier in the bulk. At this stage, the current increases exponentially with the strain [4]. This means a decreased distance between adjacent molecules, which results in some trapped carriers being movable and then joining in the conductivity. A larger strain will lead to better conduction. The remarkable enhanced carrier transport will result in a relative insufficiency of carrier injection. Thus the carrier injection becomes the main factor of current limitation. This causes the current to increase more slowly on the same variation of strain, even making it saturate at a high current density.

In an organic device, a well-accepted mechanism on carrier injection is reported by Parker [22], which predicted

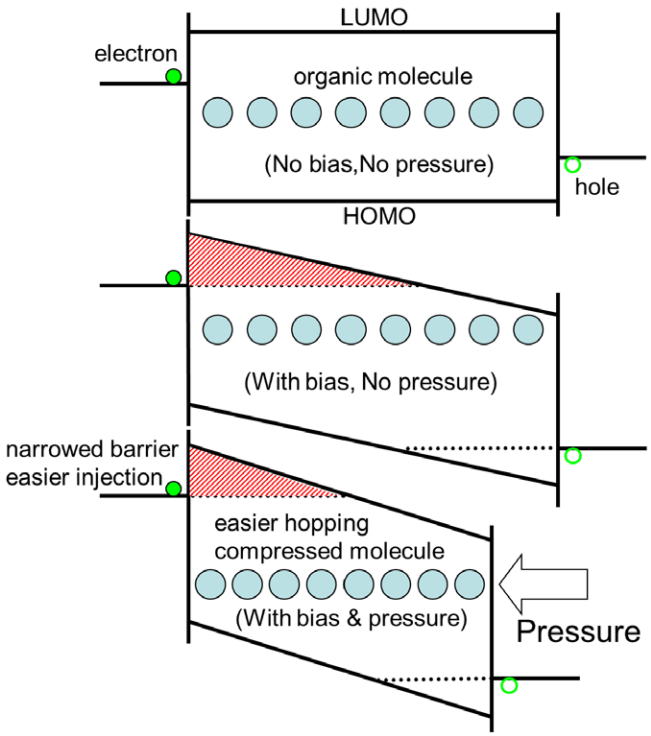

Figure 7. The compressed molecules and the narrowed barrier of carrier injection under pressure.

the current in the Fowler–Nordheim equation:

$$I \propto F^2 \mathrm{e}^{-\frac{k}{F}} \qquad \text{or} \qquad I \propto V^2 t^{-2} \mathrm{e}^{-\frac{kt}{V}}. \tag{18}$$

Here I is the current, F is the electric field strength, k is a parameter that depends on the barrier height, and t is the thickness that depends on the strain of the organic film. As shown in figure 7, the carrier injection is described such that an electron overcomes and passes through a triangle energy barrier [22]. The height is the energy difference between the Fermi level of the electrode and the LUMO of the organic film, which keeps constant in the pressure sensing. The possibility of a carrier passing through the barrier is proportional to exponential function of the barrier's area. The width is the barrier's width, which changes proportionally to the intermolecular distance in the organic film. F mostly depends on the applied voltage and the varying thickness. Therefore, as seen in equation (18), the current is mainly an exponential function of strain, which is similar to what the Miller–Abrahams model has predicted. So we can use the Miller–Abrahams model in the carrier injection at the organic/electrode interface.

Figure 8 showed the experimental (data point) and simulation (line) results of MEH-PPV and Alq (see the inset) based on the above model. It can be seen that the current is more sensitive when the strain is little. The sensitivity increases when the working voltage increases from 0.2 to 1 V, and decreases when it changes from 1 to 5 V. All the curves, except for the curve of 0.2 V, show a bending at the big strain. This may due to the limited carrier injection at high current density, and the carrier injection is sufficient at 0.2 V, since the current density is too small for its injection limit.

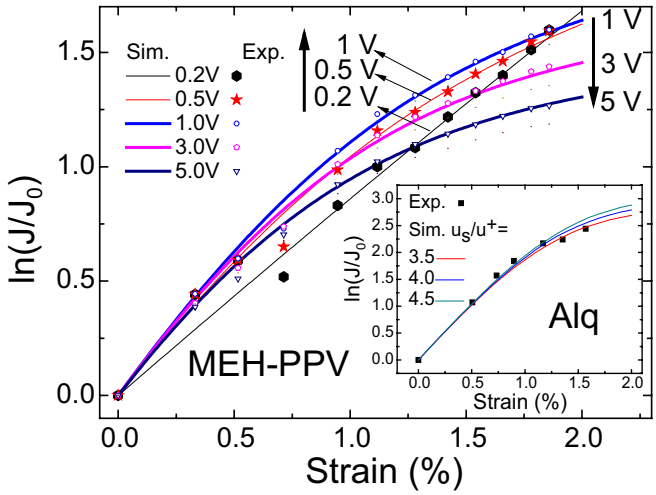

Figure 8. The experimental and simulation results of MEH-PPV device and the results of Alq device in the inset.

When the current density is bigger, the carrier injection limit is more serious, and thus the curves bend more and more. So the present MEH-PPV device works at 1 V with the highest sensitivity. Comparing the piezoresistive performances of MEH-PPV and Alq devices in figure 8 and the inset, we can see under the same strain, the relative increment of current in Alq device is larger than that in MEH-PPV device. For example, at the same strain of 2%, $\ln(J/J_0)$ is about 2.5 in Alq device, while it is about 1.5 in MEH-PPV device. This means the relative increment of current in an Alq device is about 5 [exp(2.5/1.5)] times the value of that in an MEH-PPV device. In figure 4, it can be found that MEH-PPV is softer than Alq when the load curves of MEH-PPV and Alq are compared. This means MEH-PPV can be compressed more easily, e.g., to obtain the same strain of 2%, MEH-PPV film needs a force of only ∼0.125 mN, while Alq film needs a ten times bigger force (∼1.25 mN). In generally, comparing the presented MEH-PPV device with the Alq device, the first has a higher sensitivity of current change to the applied pressure.

4. Conclusions

In summary, we measured the piezoresistive properties of the device ITO/MEH-PPV/ITO and ITO/Alq/Al, together with the stress–strain curves of both organic films. We proposed that the current is dominated by the carrier transport at the initial stage of the pressure sensing, while the current density is low. And then it should be dominated by the carrier injection at the next stage if the current density is too big to be sufficiently injected. The working voltage with the highest sensitivity is 1 V in the presented MEH-PPV device.

Acknowledgments

This work was financially supported by the Shanghai Commission of Science and Technology under Grant 12ZR1402400, the National Natural Science Foundation of China under Grant 11134002, and the Ministry of Education of People's Republic of China.

References

[1] Samara G A and Drickamer H G 1962 *J. Chem. Phys.* **37** 474
[2] Liu C Y and Bard A J 2002 *Nature* **418** 162
[3] Chandrasekhar M, Guha S and Graupner W 2001 *Adv. Mater.* **13** 613
[4] Zhong G Y, Liu Y, Song J, Zhao Q and Li Y S 2008 *J. Phys. D: Appl. Phys.* **41** 205106
[5] Zhong G Y, Zhang Y Q and Cao X A 2009 *IEEE Electron Dev. Lett.* **30** 1137
[6] Jiang Z Y and Cao X A 2010 *Appl. Phys. Lett.* **97** 203304
[7] Smith C S 1954 *Phys. Rev.* **94** 42
[8] Maheshwari V and Saraf R 2008 *Angew. Chem. Int. Edn Engl.* **47** 7808
[9] Roichman Y, Preezant Y and Tessler N 2004 *Phys. Status Solidi* a **201** 1246
[10] Miller A and Abrahams E 1960 *Phys. Rev.* **120** 745
[11] Marcus R A 1993 *Rev. Mod. Phys.* **65** 599
[12] Noolandi J 1977 *Phys. Rev.* B **16** 10
[13] Zhou J, Zhou Y C, Zhao J M, Wu C Q, Ding X M and Hou X Y 2007 *Phys. Rev.* B **75** 153201
[14] Tessler N, Preezant Y, Rappaport N and Roichman Y 2009 *Adv. Mater.* **21** 2741
[15] Bässler H 1993 *Phys. Status Solidi* b **175** 15
[16] Brinkmann M, Gadret G, Muccini M, Taliani C, Masciocchi N and Sironi A 2000 *J. Am. Chem. Soc.* **122** 5147
[17] Katakura R and Koide Y 2006 *Inorg. Chem.* **45** 15
[18] Paasch G, Nesterov A and Scheinert S 2003 *Synth. Met.* **139** 425
[19] Blom P W, de Jong M J M and Vleggaar J J M 1996 *Appl. Phys. Lett.* **68** 3308
[20] Rakhmanova S V and Conwell E M 2000 *Appl. Phys. Lett.* **76** 25
[21] Chen C H and Meng H F 2005 *Appl. Phys. Lett.* **86** 201102
[22] Parker I D 1994 *J. Appl. Phys.* **75** 1656